Belousov-Zhabotinsky liquid marbles in robot control

Michail-Antisthenis Tsompanas[a], Claire Fullarton[a], Andrew Adamatzky[a]

[a]*Unconventional Computing Laboratory,*
University of the West of England, Bristol, BS16 1QY, UK

Abstract

We show how to control the movement of a wheeled robot using on-board liquid marbles made of Belousov-Zhabotinsky solution droplets coated with polyethylene powder. Two stainless steel, iridium coated electrodes were inserted in a marble and the electrical potential recorded was used to control the robot's motor. We stimulated the marble with a laser beam. It responded to the stimulation by pronounced changes in the electrical potential output. The electrical output was detected by the robot. The robot changed its trajectory in response to the stimulation. The results open new horizons for applications using oscillatory chemical reactions in robotics.

Keywords: robot, Belousov-Zhabotinsky medium, liquid marble

1. Introduction

Belousov-Zhabotinsky (BZ) reaction is an oscillatory chemical reaction, a model of an excitable non-linear medium [11, 35, 28]. A non-stirred BZ solution exhibits interesting spatio-temporal patterns as a result of chemical excitation wave-fronts, e.g. target waves, spiral waves and localised wave-fragments. The oxidation waves have been used for image processing and computation. Wet electronics and computing circuits prototyped in BZ medium include chemical diodes [23], Boolean gates [38, 36], neuromorphic architectures [18, 16, 44, 39, 19] and associative memory [40, 41], wave-based counters [17], arithmetic circuits [8, 42, 53, 43, 20]. Moreover, as BZ proved to be a light-sensitive chemical system, it was employed in several image processing studies [26, 32, 33, 49].

BZ controllers for robots have been studied theoretically in the models of excitable automata lattices supplied with propulsive cilia [4]. A chemical processor to navigate a robot around obstacles in an arena has been prototyped in [2]. This processor, however, required images of the whole experimental arena to be prepared by a human operation in an off-line mode. The first real time BZ controller for a robot was designed and prototyped in [3]. In this case, a thin layer of BZ medium contained within a Petri dish was mounted onto a wheeled robot. Direction towards a source of stimulation was inferred, via an optical interface, from the 2D patterns of oxidation wave-fronts. Another example a BZ robotic controller is the closed loop control of a robotic hand with a thin layer BZ reactor [51]. The closed loop is achieved with photo-sensors placed underneath the Petri dish where the excitation of the BZ medium occurs from the movement of the robotic fingers. The way the robotic fingers react, in turn, is controlled by a micro-controller receiving data from the photo-sensors. The developed hybrid system was able to deliver highly complex behaviour by using just three sensors and three of the five fingers. Recently, the use of BZ gels was proposed to assemble millimetre-sized soft robots that exhibit photo-taxis, while not using any other kind of device to move around [10]. With the simulation of the chemical, along with the mechanical motion of the gels, their capabilities were unveiled. These worm-like gels can follow complicated routes based on different intensities of light, perform periodic movement resembling cilia and self-organise in groups.

Previously, the BZ medium has been utilised as an isolated system that needs specialised interfaces and data processing tools. We propose a hybrid system where the chemical system provides information to conventional electronics that control the movement of the robotic system through a direct electrical connection. Thus, this is a further step towards the final goal of autonomous next generation soft robots.

Previous prototypes of BZ controllers employed BZ in a Petri dish, which posed difficulties with manipulation and portability of the prototypes [3, 51]. Therefore, to overcome these difficulties, we decided to encapsulate ferroin-

2

catalysed BZ solution in a liquid marble. A liquid marble (LM) is a microlitre liquid droplet encapsulated in a hydrophobic powder coating [5]. This approach enables us to transfer and manipulate the BZ LM controller without wetting the underlying surface. Our scoping studies showed that the BZ media encapsulated in LMs exhibits 'classical' chemical excitation wave patterns, with mainly trigger waves observed [14]. The BZ media has been reported to be sensitive to illumination. Toth et al [45] experimentally demonstrated that visible light of the appropriate frequency, in their case a HeNe laser with wavelength 632.8 nm, initiates oxidation in the ferroin-catalysed BZ reaction. Moreover, visible light of different wavelengths is proved to initiate or inhibit the dynamics of ferroin- or ruthenium-catalyzed BZ medium due to the photochemical properties of the catalyst [37, 47, 24, 15, 21]. In this study, we use a laser beam to stimulate BZ LMs onboard of a Zumo robot.

The BZ LMs were mounted on and electrically interfaced with the Zumo robot [31]. The alternation in the dynamics of the reagents inside the BZ LM can be monitored potentiometrically with two iridium coated stainless steel electrode. Several paradigms of studies that use electrical potential to monitor the oscillation in a BZ system were previously published [9, 15, 30]. The robot is attractive in its simplicity of design and control. It has been used previously in studying route-following by klinokinesis, inspired by the navigation skills of desert ants [25], randomised algorithm mimicking biased lone exploration in roaches [22], and the self optimisation procedure on a line-tracing application by using a evolutionary computing algorithm [52].

2. Methods

Belousov-Zhabotinsky (BZ) liquid marbles (LMs) were produced by coating droplets of BZ solution with ultra high density polyethylene (PE) powder (Sigma Aldrich, CAS 9002-88-4, Product Code 1002018483, particle size $100\mu m$). The BZ solution was prepared using the method reported by Field [12], omitting the surfactant Triton X. 18 M Sulphuric acid H_2SO_4 (Fischer Scientific), sodium bro-

3
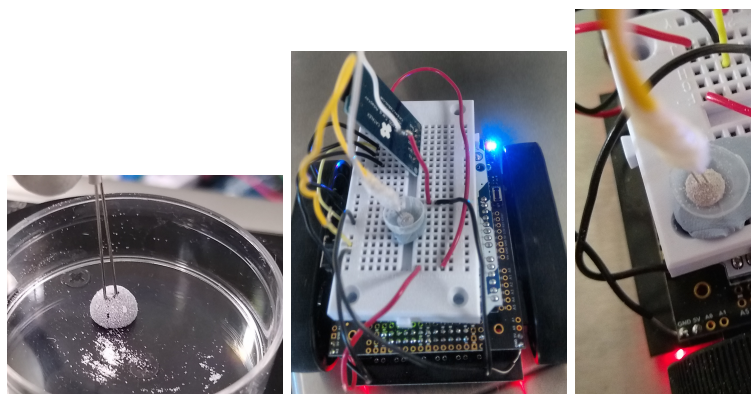
(a)   (b)   (c)
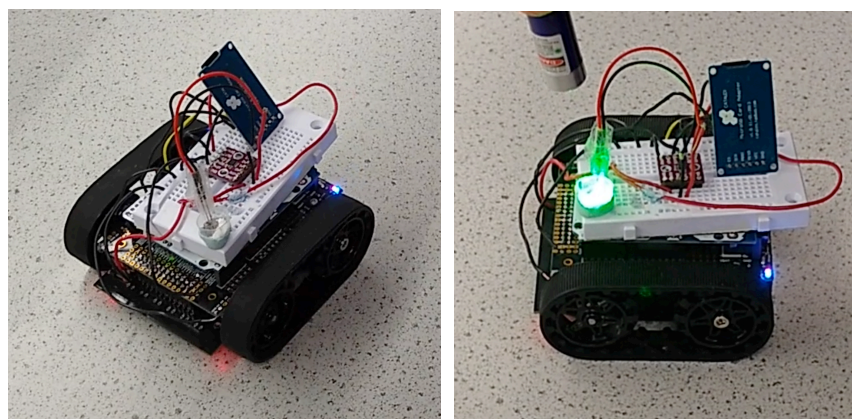
(d)   (e)

Figure 1: Experimental setup. (a) Electrical connection to record the potential of the BZ marble. (b) BZ marble rests on the robot platform. (c) Close up shot of two BZ LM on-board the robot platform. (d) Robot is controlled by BZ marble. (e) BZ LM is stimulated with laser beam.

mate $NaBrO_3$, malonic acid $CH_2(COOH)_2$, sodium bromide NaBr and $0.025\,\text{M}$ ferroin indicator (Sigma Aldrich) were used as received. Sulphuric acid ($2\,\text{ml}$) was added to deionised water ($67\,\text{ml}$), to produce $0.5\,\text{M}$ H_2SO_4, $NaBrO_3$ was added to the acid to yield $70\,\text{ml}$ of stock solution.

Stock solutions of $1\,\text{M}$ malonic acid and $1\,\text{M}$ NaBr were prepared by dissolving

1 g in 10 ml of deionised water. In a 50 ml beaker, 0.5 ml of 1 M malonic acid was added to 3 ml of the acidic $NaBrO_3$ solution. 0.25 ml of 1 M NaBr was then added to the beaker, which produced bromine. The solution was set aside until it was clear and colourless (ca. 3 min) before adding 0.5 ml of 0.025 M ferroin indicator.

BZ LMs were prepared by pipetting a $75 \mu L$ droplet of BZ solution, from a height of ca. 2 mm onto a powder bed of PE, using a method reported previously [14]. The BZ droplet was rolled on the powder bed for ca. 10 s until it was fully coated with powder.

For the initial experiments, which aimed to establish the electrical potential outputs of a BZ LM, a LM was placed in a Petri dish and pierced with two iridium coated stainless steel electrodes (Fig. 1(a)). For experiments investigating the electrical potential of a BZ LM stimulated with a laser, sub-dermal needle electrodes with twisted cables were used [1]. Electrical potential outputs were recorded with an ADC-24 high resolution data logger [2], sampling every 10 ms.

BZ LMs were mounted on the robot by rolling the LMs into plastic holders, which were subsequently attached to the robot (Fig. 1(b)) and then the LMs pierced with two iridium coated stainless steel electrodes (Fig. 1(c)).

The robot used was a Zumo robot [31], which was an off-the-shelf solution. The robot is developed as an Arduino shield to provide a convenient interface with its controller. The algorithm that governs the trajectory of the robot is loaded on the Arduino board and the electronics necessary to power the motors are accommodated on the robot shield (Fig. 1(d)). Light stimulation was performed using a green laser pointer, wavelength $532nm$, $5mW$, for ca. $10s$ (Fig. 1(e)). As previously reported [45], the reduced form of the catalyst in a ferroin-catalyzed BZ medium, shows an absorption peak at $510nm$. As a result, the choice of a wavelength of $532nm$ is reasonably close to the peak to have significant impact in the dynamics of the reagents. A human operator

---

[1] © SPES MEDICA SRL Via Buccari 21 16153 Genova, Italy
[2] Pico Technology, St Neots, Cambridgeshire, UK

has illuminated the BZ LM with a laser pen from a distance of approximately 20 cm. Using a FLIR ETS320 thermal camera with 0.06^{o}C resolution we found that the illumination does not lead to a substantial increase in temperature in the marble (even illumination for over 30 sec causes just 0.2^{o}C increase).

For the on-board recording an analogue-to-digital converter was used (ADS1118)[3].This was because the Arduino could read only positive values of an electrical potential and its resolution was limited to $4.9\,$mV. As a result, negative values can be recorded and a higher resolution (down to $0.2\,$mV) was achieved. The on-board recordings were saved on to an SD-card attached to the Arduino and started $3\,$s after the activation of the robot due to initialisation procedures. The robot is programmed with a simple algorithm to manipulate its movement in a constant way. However, this is not limiting its capabilities. Just for illustration reasons, in the experiments executed in this study, the algorithm dictates the robot to move $1.2cm$ forward (during $0.2s$) and turn to either direction at an angle of 3 degrees (during $0.2s$). As a result, the total duration of each movement of the robot is $0.4s$.

3. Results

As the oxidation wave-fronts are travelling within the BZ LM, an electrical potential that oscillates is observed in the electrodes. The dynamics of the wave-fronts and, thus, the oscillating potential are changing in response to the LM being illuminated by a laser. More specifically, one case studied was when the LM had a potential that oscillated around a negative value and was exposed to a laser beam while at the higher point of the oscillation in the positive region (Fig. 2(a)). The respond was inhibition of the oscillating output and a decrease of the oscillations' amplitude as realised in Fig. 2(a). Another case was a sudden drop of potential with no significant changing in the oscillation characteristics (Fig. 2(b)). Thus, the main difference between the two cases

---

[3]Texas Instruments Incorporated, `http://www.ti.com/lit/ds/symlink/ads1118.pdf`
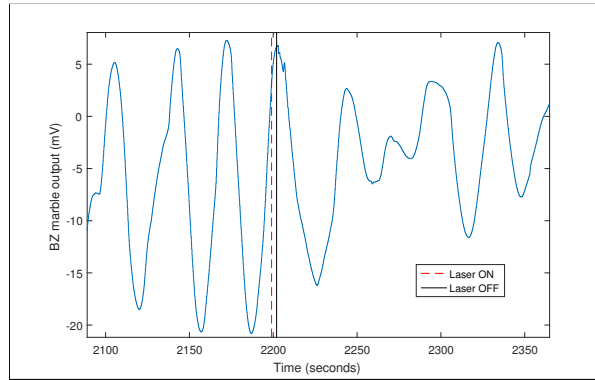
(a)
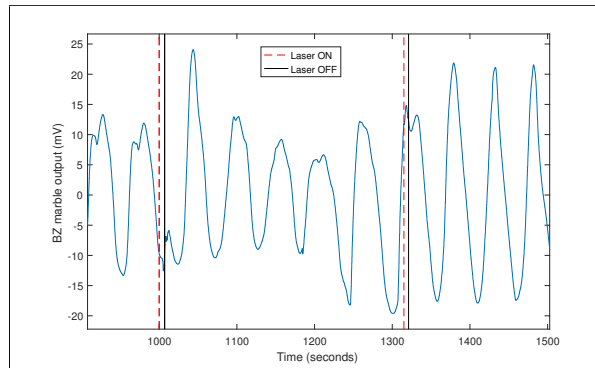
(b)

Figure 2: Dynamics of electrical potential record from BZ LMs via Pico ADC-24. Moments when the LM was illuminated with a laser are shown by vertical lines.

is that while the oscillation is heavily disturbed in Fig. 2(a) after the laser stimulation, in Fig. 2(b) after recovering from the brief drop of potential, the oscillation resumes with high peak-to-peak amplitude.

Given the aforementioned observations of the effect the laser beam causes, we developed the algorithm that would navigate the robot by taking values of the potential from the BZ LM as follows. The algorithm, loaded to the Arduino board connected to the Zumo robot, reads the outputs from a BZ LM and if the value is positive then the robot turns left. Whereas, if the value read is negative the robot turns right. In order to avoid movement when the potential output of

7

the BZ LM is too low, a condition of the absolute value being higher than 1mV was introduced. The electrical potential of the BZ LMs is read every 2 seconds and logged on an on-board SD card for further investigation.

To enhance the comprehension of the results drawn from the robot experiments, the following figures (Figs. 3-6) are encoded as described here. The asterisks represent a positive potential value of the BZ LM and, hence, a left turn of the robot. Respectively, the squares in the graphs represent a negative potential value read and, hence, a right turn of the robot. The circles represent a lower value than the minimum threshold that does not dictate any movement by the robot. The dashed vertical lines represent the time slots when the laser beam stimulating the BZ LM was on, and the solid vertical lines when the laser beam was off. The x-axis is the time in seconds and the y-axis is the voltage amplitude of the BZ LM in volts. Additionally, the trajectory of the robot for every experiment, highlighting the different directions of turning, is presented as a subfigure. Namely, the case of the robot turning left is indicated as a light grey (or green) rectangle, while the case of the robot turning right as a dark grey (or red) rectangle. The starting position of the robot is designated as the lower middle part of the depicted arena in the corresponding illustrations for all experiments.

For the first experiment involving the robot, there was no stimulation with the laser beam. The potential output and the movement of the robot is depicted in Fig. 3. The potential output oscillates around zero. Thus, the robot moves either towards the right direction or towards the left direction. Given that sampling points are equally distributed between negative and positive values, the robot is moving roughly towards a given direction.

The following experiments were executed to examine the effect of the stimulation of the BZ LM with a laser beam. Note here that the majority of the periods of illumination were approximately 10 seconds. Moreover, the initiation of the illumination was chosen randomly to avoid any correlation with the periods of oscillation of the BZ LMs observed on previously presented experiments. The amplitude of the potential output of the BZ LM was not known to the hu-
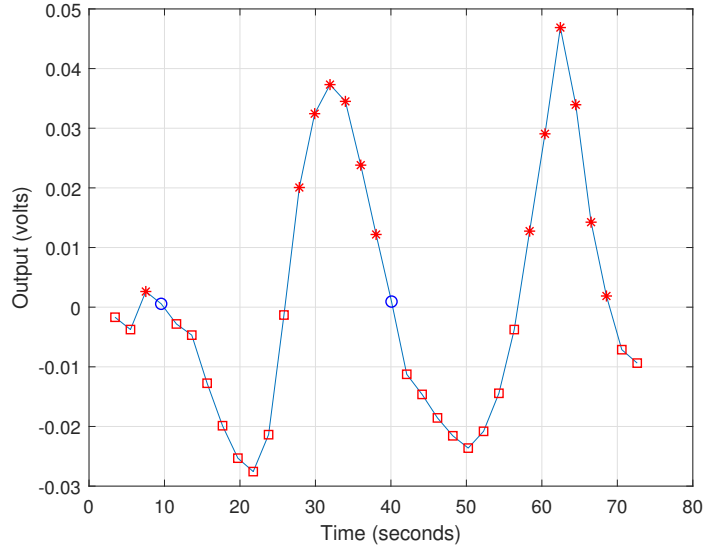
(a)
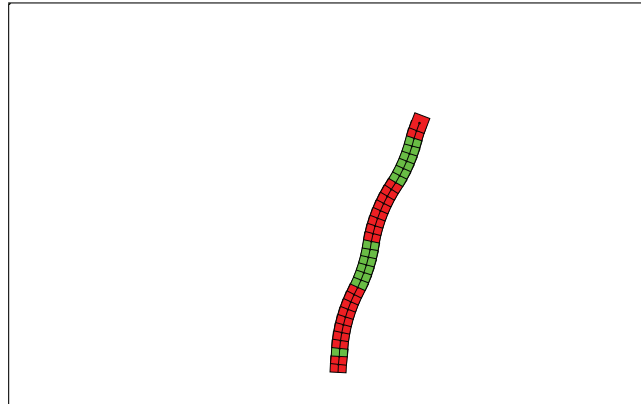
(b)

Figure 3: Results of the first experiment (with no stimulation using the laser beam). (a) Voltage output of the BZ LM and (b) trajectory of the robot. Supplementary Video BZRobot19.mp4 at [46].

man operator during the experiment, as these data were saved on the on-board SD card and extracted only after the experiment was executed.

The second experiment with the robot was executed with the interaction of

the BZ LM with a laser beam. As illustrated in the results from that experiment (Fig. 4) the effects of the laser beam are altering the normal oscillation (as depicted in Fig. 3) of the BZ LM. The first point of stimulation (at the 10th second) hinders the oscillation and maintains the potential values in the positive area. As a result the robot keeps moving towards a left direction. The second moment of stimulation (at the 32nd second) reactivates the oscillation around zero and, thus, forcing the robot to swing its way towards a generally straight direction. However, the two remaining stimulations with the laser does not seem to have a detectable effect on the output potential of the BZ LM.

The results of the third experiment are featured in Fig. 5. Despite the fact that all the incidents of stimulation with the laser beam have a clear effect on the oscillation and the short term amplitude of the potential, the robot moves only by turning left. The robot actually is working its way around a circle (anticlockwise), due to the fact that the potential of the BZ LM was not allowed to reach negative values, possible due to repeated initiation of oxidation wave-fronts by laser illumination.

For the final experiment the results are depicted in Fig. 6. Here, the output was initially oscillating within negative values. After the first stimulation with the laser beam, the potential output is constantly increasing and reaches positive values. As a result the robot stops moving in a clockwise direction and starts an anticlockwise turn. The oscillation is now around zero. However the second stimulation hinders the oscillation, with values of electrical potential remaining positive longer and, thus, the robot moves in an anticlockwise turn once more.

In order to give a sense of the distribution of trajectories that are possible, a comparison is presented of two different experiments, one that results to the robot moving towards an overall left direction and another for an overall right direction. The results of the second (Fig. 4) and fourth (Fig. 6) experiments were overlaid. In Fig. 7(a) the comparison of the voltage outputs for the two experiments was drawn in the same axes. Furthermore, in Fig. 7(b) the two trajectories are depicted, given that the robot would start from the same point in the arena. For the second experiment, the robot reaches the position in the

10
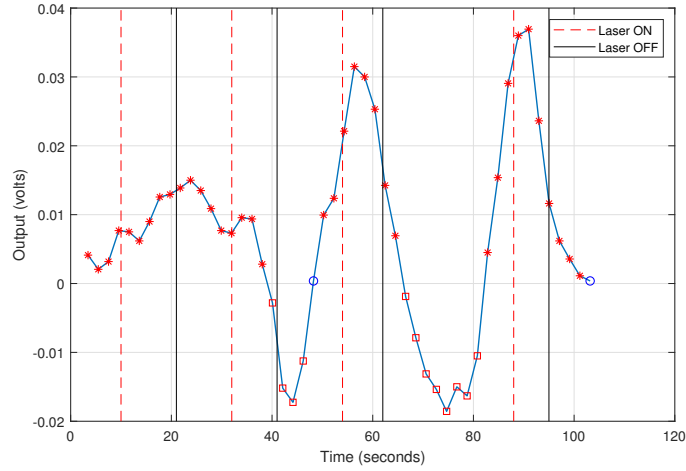
(a)
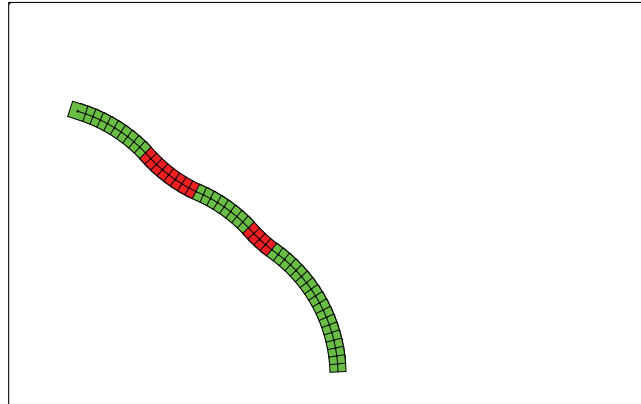
(b)

Figure 4: Results of the second experiment (with stimulation with the laser beam). (a) Voltage output of the BZ LM and (b) trajectory of the robot. Supplementary Video BZRobot20.mp4 at [46].

left of the starting point, while for the fourth experiment, the robot reaches the position in the right of the starting point.

The electrodes are penetrating through the BZ LM and the plastic container onboard of the robot. Consequently, the BZ LM is not able to move freely in the

11
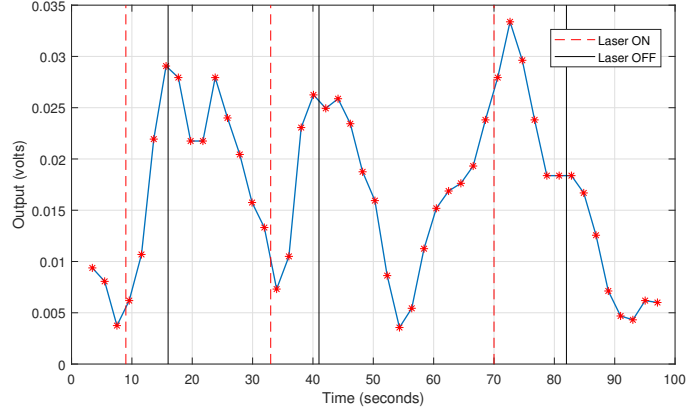
(a)
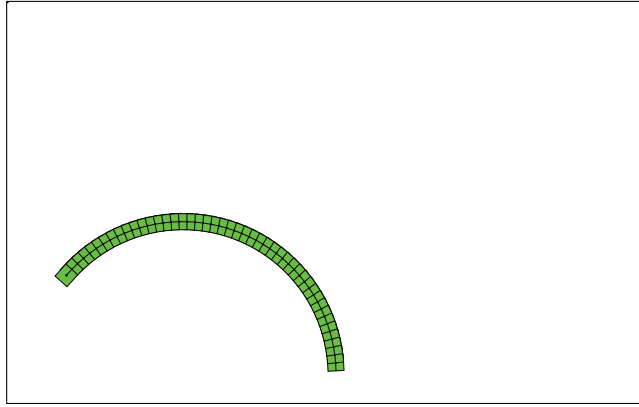
(b)

Figure 5: Results of the third experiment (with stimulation with the laser beam). (a) Voltage output of the BZ LM and (b) trajectory of the robot. Supplementary Video BZRobot21.mp4 at [46].

plastic container. Given that the oscillation period of the potential is similar in experiments without movement (Fig. 2) and with movement (Figs. 3 to 6), the vibrations from the robot seem not to be enough to characterize the LM as a well-mixed system. As a result, the BZ LM can be considered as a distributed-parameter system with local concentration gradients.

All the electrical potential values saved on the on-board SD card of the
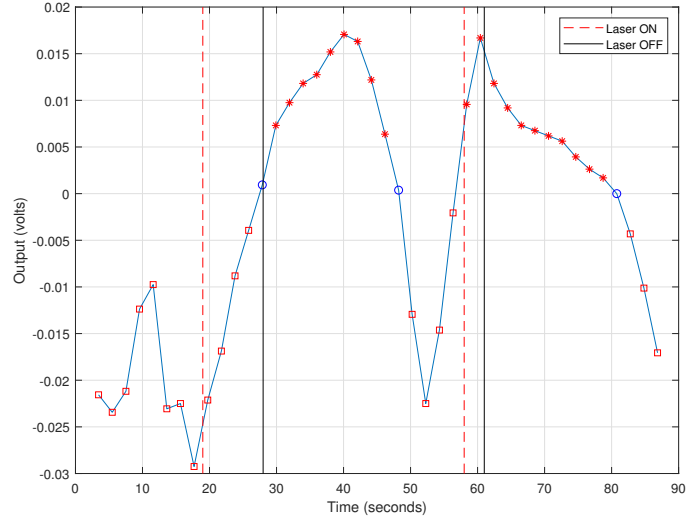
(a)
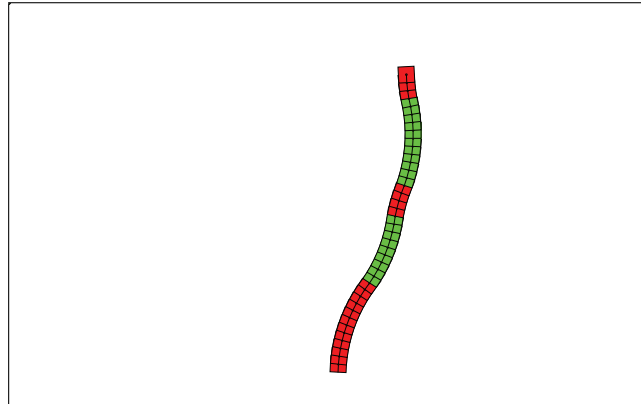
(b)

Figure 6: Results of the fourth experiment (with stimulation with the laser beam). (a) Voltage output of the BZ LM and (b) trajectory of the robot. Supplementary Video BZRobot23.mp4 at [46].

Arduino system were congregated and investigated. The resulted data set was used to produce the histogram presented in Fig. 8. Moreover, a fitted normal distribution of the appearances of each batch of electrical potential was plotted
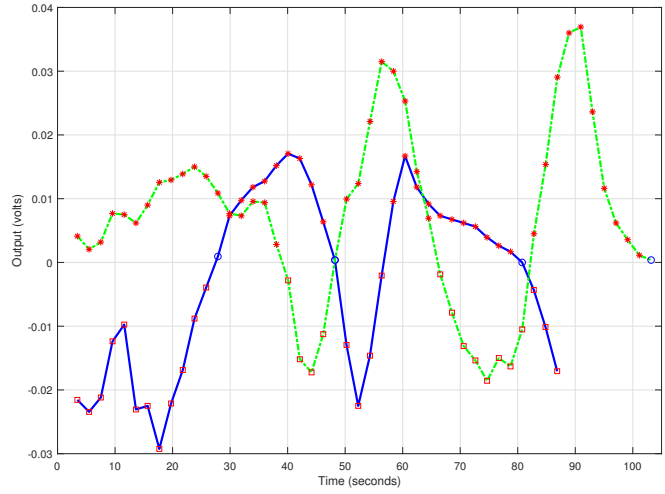
(a)
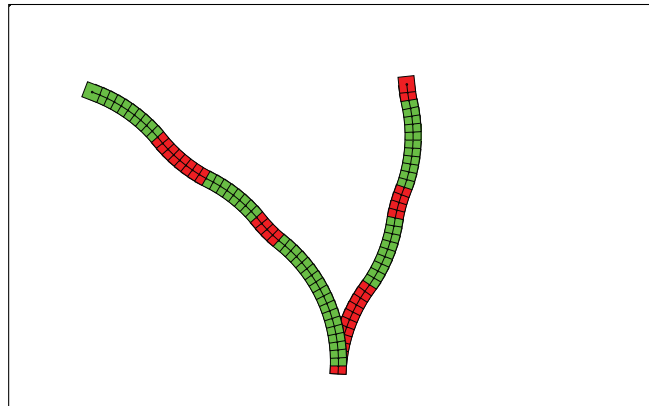
(b)

Figure 7: Comparison of second and fourth experiments. (a) Overlay of voltage output of the BZ LMs (second experiment in green dotted line and fourth experiment in blue solid line) and (b) trajectories of the robot starting from the same point.

in Fig. 8. The mean value is 0.006 and the standard deviation 0.0159. Thus, the definition of assigning left or right turns with values around zero (which is close to the mean of 0.006) provides an almost evenly distributed motion towards both sides.

14
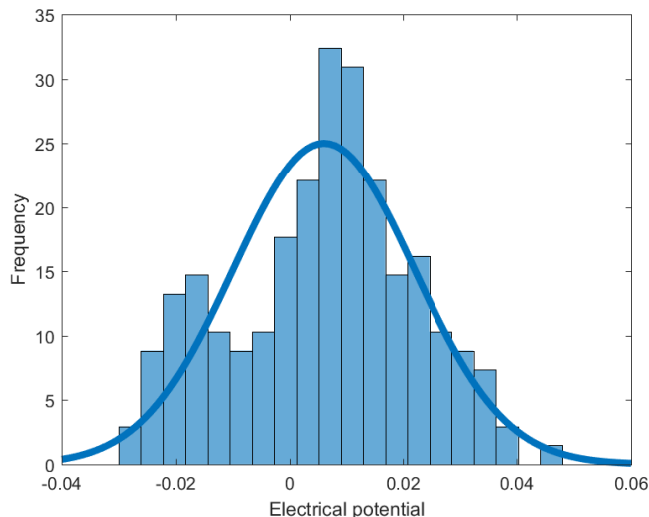
Figure 8: Histogram and fitted normal distribution of appearances of electrical potential of the BZ LM for all four experiments.

4. Discussions

This work demonstrates that the BZ reaction can be directly incorporated into the electronic circuitry of a controller for a robot. Limitations imposed by earlier prototypes of liquid phase controllers, where robots were restricted to forward speeds of ca. 1cm/s and rotation speeds of ca. 1 degree/s [3], were alleviated. The additional benefits of the BZ LM system were that no optical interfaces were required to monitor the BZ LM controller and the geometries of the oxidation wave-fronts no longer need to be analysed. Hardware and software used in previous versions of the robot [3, 51] (a light placed underneath the reaction contained within a Petri dish, a serial connection to a PC and image processing algorithms) are not necessary as the BZ LMs are electrically connected to the micro-controller that delivers the trajectory of the robot. This reduction in the complexity of the controller system shows progress towards future unconventional and soft robotics.

By encapsulating the BZ solution droplets in hydrophobic powder to form

15

LMs, made the controllers re-configurable. In principle, it would be possible to mount as many BZ marbles as desired on-board of a robot and allow the LM ensembles to process information about the local environment and potentially make decisions based on the fusions of many stimuli. The properties of LMs can be tailored for a variety of applications by altering the encapsulated liquid and / or the powder coating [7, 6, 13, 27, 29, 34]. This means LMs can be prepared to enable them to be manipulated using electrical and magnetic fields, in addition to mechanical manipulation. Thus, robotic BZ LM controllers can be reconfigured on-the-fly, during the robot is in motion. Another aspect of future work is replacing the BZ LM with other unconventional sensors (like slime mould [1, 50]), which will not require any complicated action concerning the configuration of the robot. Furthermore, the results presented here can be a stepping stone towards the combination of electrical connections of BZ LMs stimulated by laser beams on an array, similar to the BZ micro-droplet arrays reported in [48].

This is an initial study towards the control of robots with chemical reaction-diffusion systems through an electrical connection. It is a contribution in bringing important improvement in prototyping wet robotics bearing complex dynamics. Excluding the results of the third experiment (presented in Fig. 5, where no alternation of the initial trajectory was observed), the stimulation of the BZ LM controller was followed by the event of the robot changing its trajectory (either turning the other way or stop turning) during the illumination period or shortly after it (maximum of 8 seconds) for 67% of the trials. However, the simplicity of the algorithm dictating the trajectory is noteworthy. Only the sign of the voltage of the BZ LM is considered. As a consequence more complicated algorithms are expected to produce higher accuracy of the control on the movement of the robot and will be studied in future experiments.

Finally, the short time of the experiments with the BZ LM mounted on the robot are not because of reagents depletion, but in order to illustrate more efficiently the reaction of the marble to laser illumination. In fact the same BZ LM was used for all experiments.

Acknowledgements

Data availability

Videos and snapshots of experiments can be found at [46].

References

[1] Andrew Adamatzky. Slime mould tactile sensor. *Sensors and Actuators B: Chemical*, 188:38 – 44, 2013.

[2] Andrew Adamatzky, Benjamin de Lacy Costello, Chris Melhuish, and Norman Ratcliffe. Experimental reaction–diffusion chemical processors for robot path planning. *Journal of Intelligent and Robotic Systems*, 37(3):233–249, 2003.

[3] Andrew Adamatzky, Benjamin de Lacy Costello, Chris Melhuish, and Norman Ratcliffe. Experimental implementation of mobile robot taxis with onboard Belousov–Zhabotinsky chemical medium. *Materials Science and Engineering: C*, 24(4):541–548, 2004.

[4] Andrew Adamatzky and Chris Melhuish. Phototaxis of mobile excitable lattices. *Chaos, Solitons & Fractals*, 13(1):171–184, 2002.

[5] Pascale Aussillous and David Quéré. Liquid marbles. *Nature*, 411(6840):924, 2001.

[6] Edward Bormashenko. New insights into liquid marbles. *Soft Matter*, 8(43):11018–11021, 2012.

[7] Edward Bormashenko. Liquid marbles, elastic nonstick droplets: From minireactors to self-propulsion. *Langmuir*, 33(3):663–669, 2017.

[8] Ben De Lacy Costello, Andy Adamatzky, Ishrat Jahan, and Liang Zhang. Towards constructing one-bit binary adder in excitable chemical medium. *Chemical Physics*, 381(1):88–99, 2011.

[9] Michael F. Crowley and Richard J. Field. Electrically coupled belousov-zhabotinskii oscillators: Experimental observation of chaos in a chemical system and identification of its source in the field-noyes equations. In Hans G. Othmer, editor, *Nonlinear Oscillations in Biology and Chemistry*, pages 68–97, Berlin, Heidelberg, 1986. Springer Berlin Heidelberg.

[10] Pratyush Dayal, Olga Kuksenok, and Anna C Balazs. Directing the behavior of active, self-oscillating gels with light. *Macromolecules*, 47(10):3231–3242, 2014.

[11] Irving R Epstein and Kenneth Showalter. Nonlinear chemical dynamics: oscillations, patterns, and chaos. *The Journal of Physical Chemistry*, 100(31):13132–13147, 1996.

[12] Richard J Field and Arthur T. Winfree. Travelling waves of chemical activity in the Zaikin-Zhabotinskii-Winfree reagent. *Journal of Chemical Education*, 56(11):754, 1979.

[13] Syuji Fujii, Shin Ichi Yusa, and Yoshinobu Nakamura. Stimuli-Responsive Liquid Marbles: Controlling Structure, Shape, Stability, and Motion. *Adv. Funct. Mater.*, 26(40):7206–7223, 2016.

[14] Claire Fullarton, Thomas C Draper, Neil Phillips, Ben PJ Costello, and Andrew Adamatzky. Belousov-zhabotinsky reaction in liquid marbles. *arXiv preprint arXiv:1806.07181*, 2018.

[15] V Gáṣpár, Gy Bazsa, and MT Beck. The influence of visible light on the beloasoy-zhabotinskii oscillating reactions applying different catalysts. *Zeitschrift für Physikalische Chemie*, 264(1):43–48, 1983.

[16] Pier Luigi Gentili, Viktor Horvath, Vladimir K Vanag, and Irving R Epstein. Belousov-Zhabotinsky "chemical neuron" as a binary and fuzzy logic processor. *IJUC*, 8(2):177–192, 2012.

[17] J Gorecki, K Yoshikawa, and Y Igarashi. On chemical reactors that can count. *The Journal of Physical Chemistry A*, 107(10):1664–1669, 2003.

[18] Jerzy Gorecki and Joanna Natalia Gorecka. Information processing with chemical excitations–from instant machines to an artificial chemical brain. *International Journal of Unconventional Computing*, 2(4), 2006.

[19] Gerd Gruenert, Konrad Gizynski, Gabi Escuela, Bashar Ibrahim, Jerzy Gorecki, and Peter Dittrich. Understanding networks of computing chemical droplet neurons based on information flow. *International journal of neural systems*, 25(07):1450032, 2015.

[20] Shan Guo, Ming-Zhu Sun, and Xin Han. Digital comparator in excitable chemical media. *International Journal Unconventional Computing*, 2015.

[21] I Hanazaki, Y Mori, T Sekiguchi, and Gy Rábai. Photo-response of chemical oscillators. *Physica D: Nonlinear Phenomena*, 84(1-2):228–237, 1995.

[22] Charles Hart, EJ Kreinar, David Chrzanowski, Kathryn A Daltorio, and Roger D Quinn. A low-cost robot using omni-directional vision enables insect-like behaviors. In *Robotics and Automation (ICRA), 2015 IEEE International Conference on*, pages 5871–5878. IEEE, 2015.

[23] Yasuhiro Igarashi and Jerzy Gorecki. Chemical diodes built with controlled excitable media. *IJUC*, 7(3):141–158, 2011.

[24] Sándor Kádár, Takashi Amemiya, and Kenneth Showalter. Reaction mechanism for light sensitivity of the ru (bpy) 32+-catalyzed belousov- zhabotinsky reaction. *The Journal of Physical Chemistry A*, 101(44):8200–8206, 1997.

[25] Aleksandar Kodzhabashev and Michael Mangan. Route following without scanning. In Stuart P. Wilson, Paul F.M.J. Verschure, Anna Mura, and Tony J. Prescott, editors, *Biomimetic and Biohybrid Systems*, pages 199–210, Cham, 2015. Springer International Publishing.

[26] L Kuhnert, KI Agladze, and VI Krinsky. Image processing using light-sensitive chemical waves. *Nature*, 337(6204):244, 1989.

[27] G. McHale and M. I. Newton. Liquid marbles: topical context within soft matter and recent progress. *Soft Matter*, 11(13):2530–2546, 2015.

[28] Alexander S Mikhailov and Kenneth Showalter. Control of waves, patterns and turbulence in chemical systems. *Physics Reports*, 425(2-3):79–194, 2006.

[29] Chin Hong Ooi and Nam Trung Nguyen. Manipulation of liquid marbles. *Microfluid. Nanofluidics*, 19(3):483–495, 2015.

[30] Valery Petrov, Vilmos Gaspar, Jonathan Masere, and Kenneth Showalter. Controlling chaos in the belousovzhabotinsky reaction. *Nature*, 361(6409):240, 1993.

[31] Pololu Corporation. *Pololu Zumo Shield for Arduino User's Guide*, 2016 (accessed July 16, 2018). `https://www.pololu.com/docs/pdf/0J57/zumo_shield_for_arduino.pdf`.

[32] NG Rambidi, TO-O Kuular, and EE Makhaeva. Information-processing capabilities of chemical reaction–diffusion systems. 1. belousov–zhabotinsky media in hydrogel matrices and on solid supports. *Advanced Materials for Optics and Electronics*, 8(4):163–171, 1998.

[33] NG Rambidi, KE Shamayaev, and G Yu Peshkov. Image processing using light-sensitive chemical waves. *Physics Letters A*, 298(5-6):375–382, 2002.

[34] Ondřej Rycheckỳ, Monika Majerská, Vlastimil Král, František Štěpánek, and Jitka Čejková. Spheroid cultivation of HT-29 carcinoma cell line in liquid marbles. *Chemical Papers*, pages 1–9, 2017.

[35] Francesc Sagués and Irving R Epstein. Nonlinear chemical dynamics. *Dalton transactions*, 7:1201–1217, 2003.

[36] Jakub Sielewiesiuk and Jerzy Górecki. Logical functions of a cross junction of excitable chemical media. *The Journal of Physical Chemistry A*, 105(35):8189–8195, 2001.

[37] O Steinbock and SC Müller. Multi-armed spirals in a light-controlled excitable reaction. *International Journal of Bifurcation and Chaos*, 3(02):437–443, 1993.

[38] Oliver Steinbock, Petteri Kettunen, and Kenneth Showalter. Chemical wave logic gates. *The Journal of Physical Chemistry*, 100(49):18970–18975, 1996.

[39] James Stovold and Simon OKeefe. Simulating neurons in reaction-diffusion chemistry. In *International Conference on Information Processing in Cells and Tissues*, pages 143–149. Springer, 2012.

[40] James Stovold and Simon OKeefe. Reaction–diffusion chemistry implementation of associative memory neural network. *International Journal of Parallel, Emergent and Distributed Systems*, pages 1–21, 2016.

[41] James Stovold and Simon OKeefe. Associative memory in reaction-diffusion chemistry. In *Advances in Unconventional Computing*, pages 141–166. Springer, 2017.

[42] Ming-Zhu Sun and Xin Zhao. Multi-bit binary decoder based on Belousov-Zhabotinsky reaction. *The Journal of chemical physics*, 138(11):114106, 2013.

[43] Ming-Zhu Sun and Xin Zhao. Crossover structures for logical computations in excitable chemical medium. *International Journal Unconventional Computing*, 2015.

[44] Hisako Takigawa-Imamura and Ikuko N Motoike. Dendritic gates for signal integration with excitability-dependent responsiveness. *Neural Networks*, 24(10):1143–1152, 2011.

[45] Rita Tóth, Vilmos Gáspár, Andrew Belmonte, Megan C O'Connell, Annette Taylor, and Stephen K Scott. Wave initiation in the ferroin-catalysed belousov–zhabotinsky reaction with visible light. *Physical Chemistry Chemical Physics*, 2(3):413–416, 2000.

[46] Michail-Antisthenis Tsompanas, Claire Fullarton, and Andrew Adamatzky. Videos of a robot controlled by Belousov-Zhabotinsky liquid marbles. Supplementary materials to the paper "Belousov-Zhabotinsky liquid marbles in robot control", October 2018. Available at `https://doi.org/10.5281/zenodo.1450868`.

[47] Vladimir K Vanag, Anatol M Zhabotinsky, and Irving R Epstein. Pattern formation in the belousov- zhabotinsky reaction with photochemical global feedback. *The Journal of Physical Chemistry A*, 104(49):11566–11577, 2000.

[48] AL Wang, JM Gold, N Tompkins, M Heymann, KI Harrington, and S Fraden. Configurable nor gate arrays from Belousov-Zhabotinsky microdroplets. *The European Physical Journal Special Topics*, 225(1):211–227, 2016.

[49] Y Wang, Y Xie, C Yuan, H Wang, and D Fu. Intelligent image sensor based on probing the evolution of redox potentials distributed in reaction–diffusion medium. *Sensors and Actuators B: Chemical*, 145(1):285–292, 2010.

[50] James G.H. Whiting, Ben P.J. de Lacy Costello, and Andrew Adamatzky. Towards slime mould chemical sensor: Mapping chemical inputs onto electrical potential dynamics of physarum polycephalum. *Sensors and Actuators B: Chemical*, 191:844 – 853, 2014.

[51] Hiroshi Yokoi, Andy Adamatzky, Ben de Lacy Costello, and Chris Melhuish. Excitable chemical medium controller for a robotic hand: Closed-loop experiments. *International Journal of Bifurcation and Chaos*, 14(09):3347–3354, 2004.

[52] Brandon Zahn, Ivan Ucherdzhiev, Julia Szeles, Janos Botzheim, and Naoyuki Kubota. Optimization of a proportional-summation-difference controller for a line-tracing robot using bacterial memetic algorithm. In *International Conference on Intelligent Robotics and Applications*, pages 362–372. Springer, 2016.

[53] Guo-Mao Zhang, Ieong Wong, Meng-Ta Chou, and Xin Zhao. Towards constructing multi-bit binary adder based on Belousov-Zhabotinsky reaction. *The Journal of chemical physics*, 136(16):164108, 2012.